

30. Graedel, T. E., Brewer, P. G. & Rowland, F. S. Panel 4. Chemistry of the air-sea interface. *Appl. Geochem.* 3, 37–48 (1988).

Supplementary Information accompanies the paper on *Nature's* website (► <http://www.nature.com/nature>).

Acknowledgements We thank A. H. Knap, A. F. Michaels, D. A. Hansell, D. K. Steinberg and C. A. Carlson for their contributions to the BATS program. We also thank the numerous technicians, graduate students, and captains and crew of the RV *Weatherbird II*, who have contributed to the success of the BATS program since 1988. W. S. Broecker, T. Takahashi, C. D. Keeling and P. G. Brewer are thanked for the use of ΣCO_2 data collected in the Sargasso Sea during 1972–86. This work was supported by the National Science Foundation and National Oceanographic and Atmospheric Administration.

Competing interests statement The authors declare that they have no competing financial interests.

Correspondence and requests for materials should be addressed to N.B. (e-mail: nick@bbsr.edu).

The role of volatiles in magma chamber dynamics

Herbert E. Huppert & Andrew W. Woods

Institute of Theoretical Geophysics, Department of Applied Mathematics and Theoretical Physics, Silver Street, Cambridge CB3 9EW, UK; and the BP Institute of Multiphase Flow, Madingley Rise, Madingley Road, Cambridge CB3 0EZ, UK

Many andesitic volcanoes exhibit effusive eruption activity¹, with magma volumes as large as 10^7 – 10^9 m^3 erupted at rates of 1 – $10 \text{ m}^3 \text{ s}^{-1}$ over periods of years or decades. During such eruptions, many complex cycles in eruption rates have been observed, with periods ranging from hours to years^{2–7}. Longer-term trends have also been observed, and are thought to be associated with the continuing recharge of magma from deep in the crust and with waning of overpressure in the magma reservoir. Here we present a model which incorporates effects due to compressibility of gas in magma. We show that the eruption duration and volume of erupted magma may increase by up to two orders of magnitude if the stored internal energy associated with dissolved volatiles can be released into the magma chamber. This mechanism would be favoured in shallow chambers or volatile-rich magmas and the cooling of magma by country rock may enhance this release of energy, leading to substantial increases in eruption rate and duration.

Consider a magma with bulk density ρ in a chamber of volume V undergoing a mass recharge rate Q_i and eruption rate Q_0 , as sketched in Fig. 1. Conservation of mass indicates that:

$$\frac{d}{dt}(\rho V) = \rho \frac{dV}{dt} + V \frac{d\rho}{dt} = Q \quad (1)$$

where $Q = Q_i - Q_0$. The density of the magma, which consists of melt, crystals and gas, can be written, in general form, as $\rho = \rho[p, T, x(T), N]$ where p is pressure, T temperature, $x(T)$ the mass fraction of crystals in the magma and N the total mass fraction of volatiles. Depending on the pressure, a fraction of these volatiles are dissolved in the magma and the remainder exist in the gaseous phase. Differentiating this expression for the density and incorporating the result into equation (1), we obtain:

$$\frac{dV}{dt} + \frac{V \partial \rho}{\rho \partial p} \frac{dp}{dt} = \frac{Q}{\rho} - \frac{V \partial \rho}{\rho \partial T} \frac{dT}{dt} \quad (2)$$

where the second term on the right-hand side represents the rate of change of volume associated with the change in density with

temperature of the magma, which includes the effects of the change of crystal content with temperature, leading to an effective thermal expansion.

It is known^{8–10} that the rate of change in volume of the chamber, dV/dt , is related to the associated rate of change in pressure, dp/dt , as a result of deformation of the surrounding rock by:

$$\frac{1}{\beta_r} \frac{dp}{dt} = \frac{1}{V} \frac{dV}{dt} \quad (3)$$

where β_r is the effective bulk modulus of the surrounding wall rock. The exact value of β_r depends on the density of microfractures in the rock, but a value of 10^{10} Pa is typical^{10,11}. Incorporating equation (3) into equation (2), we obtain:

$$V \left[\frac{1}{\beta_r} + \frac{1}{\rho} \frac{\partial \rho}{\partial p} \right] \frac{dp}{dt} = \frac{Q}{\rho} - \frac{V \partial \rho}{\rho \partial T} \frac{dT}{dt} \quad (4)$$

Thus, as expressed by equation (3), the effective bulk modulus of the compressible magma, β , is given by:

$$\frac{1}{\beta} = \frac{1}{\beta_r} + \frac{1}{\rho} \frac{\partial \rho}{\partial p} \quad (5)$$

We show here that for typical volatile-rich magmas, the second term on the right-hand side of equation (5) is much larger than the first term, which indicates that the compressibility of the saturated magma plus exsolved gas, C , defined as the inverse of the effective bulk modulus β , greatly exceeds that of the wall rock.

An explicit relationship for ρ in terms of the gas density ρ_g , the crystal density ρ_c and the melt density ρ_m is:

$$\rho = \left[\frac{n}{\rho_g} + (1-n) \left(\frac{x}{\rho_c} + \frac{1-x}{\rho_m} \right) \right]^{-1} \quad (6)$$

where, to a good approximation, the gas density follows the ideal gas law¹², $\rho_g = p/RT$, where R is the universal gas constant. We assume the exsolution of gas occurs at thermodynamic and chemical equilibrium, which is valid for the slow processes considered here^{13,14}. Thus, in our model, the exsolved volatile content, n , follows from Henry's law^{12,13,15}. This law, for water, which is frequently the dominant volatile species present, is $n = N - sp^{1/2}(1-x) \geq 0$, on the assumption that the magma is saturated, where $s = 4 \times 10^{-6} \text{ Pa}^{-1/2}$ for water vapour. This will occur at sufficiently low pressures and sufficiently high total volatile or crystal contents. Alternatively, if $sp^{1/2}(1-x) \geq N$, the magma is undersaturated and $n \equiv 0$. Analogous calculations can be made for

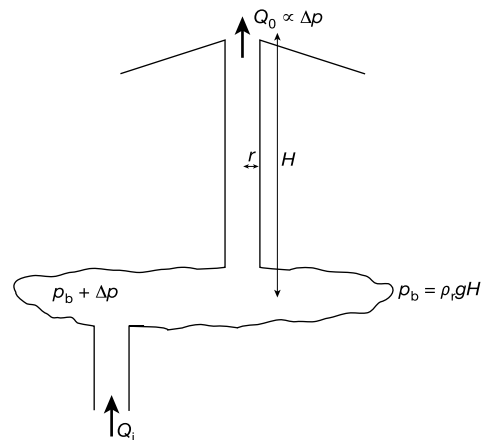


Figure 1 Schematic of magma reservoir. In the reservoir there is an overpressure Δp to a background pressure field at depth H given by $p_b = \rho_r g H$, where ρ_r is the density of the rocks above the magma chamber and g is the acceleration due to gravity. During a slow effusive eruption, through a conduit of radius r , mass is input at rate Q_i and erupted at rate Q_0 .

magmas in which the dominant volatile content is carbon dioxide. In all the calculations which follow here the crystals and melt are assumed to have bulk modulus $\beta_c = 10^{10}$ Pa (refs 10, 11).

Figure 2a and b illustrates the variation of effective compressibility $C = 1/\bar{\beta}$ with pressure for different volatile and crystal contents. As shown in Fig. 2, the depth may be related to the pressure through the lithostatic gradient. For deep, crystal-poor magmas the magma is unsaturated and hence the bulk modulus is of

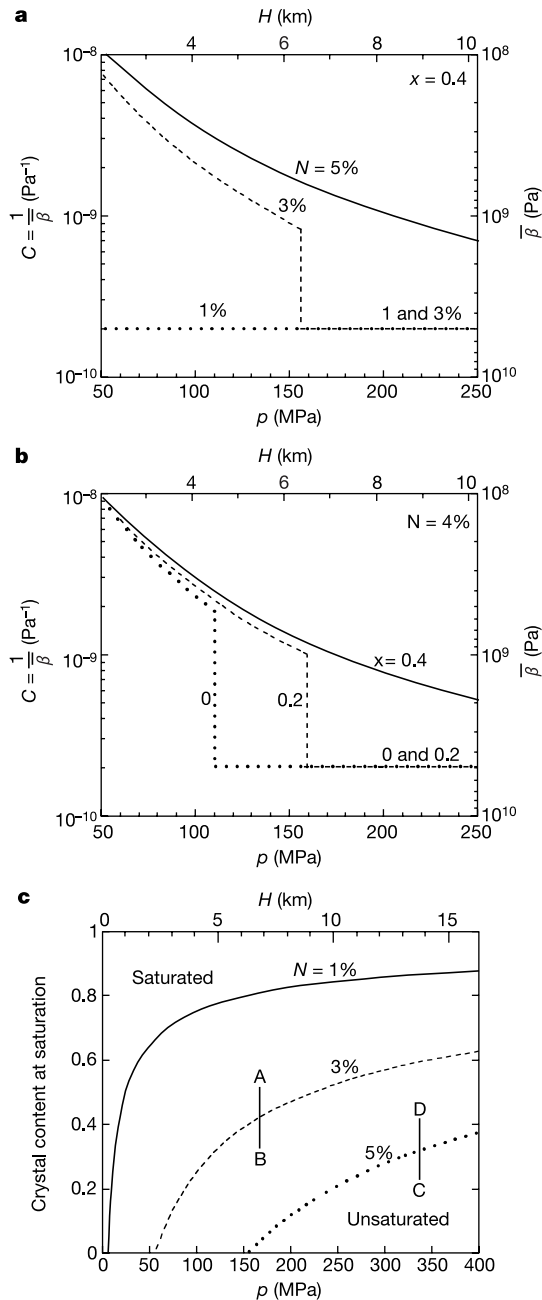


Figure 2 Magma compressibility as a function of pressure. Data are shown for various values of magma volatile content with $x = 0.4$ (a) and magma crystal content with $N = 4\%$ (b). The discontinuity in magma compressibility occurs when the magma is just saturated. When it is undersaturated there is no exsolved gas and the compressibility is the sum of the compressibility of the wall rock and that of the magma contained within the chamber. c. Critical crystal content as a function of pressure for various values of volatile content. In these calculations $s = 4 \times 10^{-6} \text{ Pa}^{-1/2}$; $\rho_c = 2,600 \text{ kg m}^{-3}$; $\rho_r = 2,500 \text{ kg m}^{-3}$; $\rho_m = 2,300 \text{ kg m}^{-3}$; $R = 462 \text{ J K}^{-1} \text{ kg}^{-1}$ and $T = 800^\circ \text{C}$ (as appropriate for silicic magma).

order 10^{10} Pa and independent of depth. For shallower systems, the magma is saturated and the much larger compressibility of the accompanying gas phase leads to a bulk modulus of order $10^8 - 10^9$ Pa. The transition in C occurs when the magma first becomes saturated. At this critical point, a small decrease in pressure leads to expansion of the mixture primarily through exsolution of relatively low-density gas, whereas a small increase of pressure can only be accommodated through compression of the liquid magma and the country rock. Figure 2c illustrates the crystallinity at which the magma first becomes saturated as a function of pressure or depth for various volatile contents. For larger crystal contents, gas is exsolved and the compressibility greatly increases (Fig. 2a, b). The greater compressibility leads to eruption of a larger mass to relieve the same overpressure and hence the duration of the resulting effusive eruption will be longer.

To evaluate the detailed response during an eruption, equations (4) and (6), being heavily nonlinear, need to be solved numerically. However, the typical change in pressure during an eruption is only of order 1–10 MPa, and Fig. 2a and b illustrates that at depths of 3–10 km, such changes in pressure lead to small variations in compressibility, typically $\leq 10\%$, except just at the saturation point (see below). As an effective approximation, we may therefore take the chamber compressibility and the chamber volume as being constant, at the mean value, during an eruption.

For given magma and flow conduit properties, the eruption rate is a function of the chamber overpressure^{16–18}. As a simple illustrative calculation, we follow ref. 19 and assume that, for a magma chamber at depth H ,

$$Q_0 = (\rho SA^2 / H\mu)\Delta p \equiv \lambda \Delta p \quad (7)$$

where S is a shape factor of about 0.1, A the conduit cross-section and μ the effective viscosity of the magma in the conduit. At

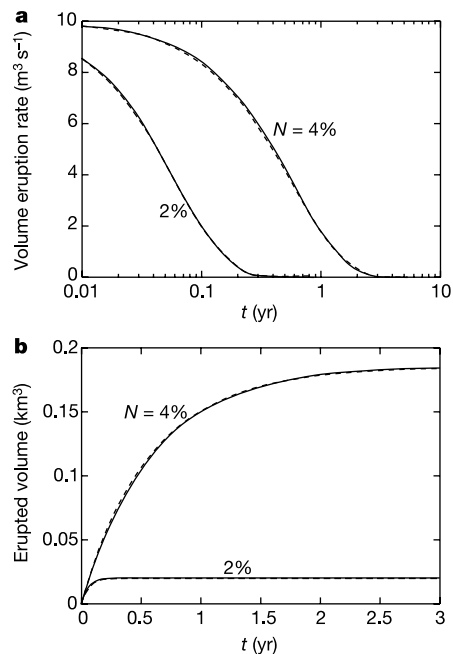


Figure 3 Eruption volume and volume eruption rate. a. Volume eruption rate Q_0 , which is proportional to the chamber overpressure Δp , as expressed in equation (7). b. Erupted volume V_e , as functions of time for magma at a depth, H , of 5 km. The calculations incorporate a crystal content $x = 0.4$ and volatile contents of 2 wt% (a typical undersaturated magma) and 4 wt% (a typical saturated magma). The conduit radius is 15 m, and dynamic viscosity $\mu = 10^7$ Pa. The chamber volume is 10 km^3 and initial chamber overpressure is 10 MPa. Solid lines show predictions of the approximate model equations (9) and (10) with $\bar{\beta} = 127.6 \text{ MPa}$, and dashed lines are numerical solutions incorporating the full variation of β .

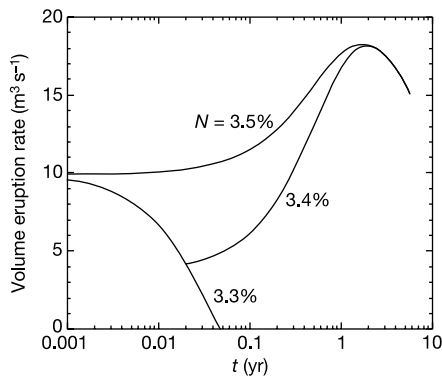


Figure 4 Variation of eruption rate for a silicic magma at a depth of 5 km with 3.5, 3.4 and 3.3 wt% volatiles, accounting for the cooling of the magma at a rate of 10^{-6} K s^{-1} according to equation (4). After less than one tenth of a year, the magma with a 3.4 wt% volatile content becomes saturated and hence much more compressible; also the chamber pressure begins to increase owing to the increasing volume of gas. This leads to an increase in the eruption rate and a much longer eruption duration and erupted mass. Magma with 3.3 wt% volatile content remains unsaturated, and has a much more rapidly waning eruption rate, while magma with 3.5 wt% volatiles is already saturated and shows a gradually increasing eruption rate with time owing to the crystallization and the associated gas release.

constant temperature, the chamber overpressure, Δp , then evolves as:

$$\frac{d\Delta p}{dt} = \{Q_i - \lambda\Delta p\}(\bar{\beta}/\rho V) \quad (8)$$

which has a solution for an eruption initiated at an overpressure Δp_0 at $t = 0$ of

$$\Delta p = \Delta p_0 \exp\left(-\frac{\lambda\bar{\beta}t}{\rho V}\right) + \left(\frac{\bar{\beta}}{\rho V}\right) \int_0^t \exp\left[-\frac{\lambda\bar{\beta}}{\rho V}(t-s)\right] Q(s) ds \quad (9)$$

As an example, for constant Q_i , equation (9) reduces to:

$$\Delta p = [\Delta p_0 - Q_i/\lambda] \exp[-\lambda\bar{\beta}t/\rho V] + (Q_i/\lambda) \quad (10)$$

whereas the volume erupted, V_e , is given by:

$$V_e = \frac{V}{\bar{\beta}}(\Delta p_0 - Q_i/\lambda) \left[1 - \exp\left(-\frac{\lambda\bar{\beta}t}{\rho V}\right)\right] + Q_i t/\rho \quad (11)$$

Figure 3 shows predictions of equations (10) and (11) for two typical eruptions (with $Q_i = 0$). This illustrates how the presence of volatiles in the magma reservoir leads to an increase in eruption time and erupted volume by a factor of 30 for the particular chosen conditions. We note that the timescale of the eruption $\tau = \rho V/\lambda\bar{\beta}$ and that the total erupted volume $V_e = V\Delta p_0/\bar{\beta}$. Both of these increase with increasing exsolved volatile content, through the factor $1/\bar{\beta}$, as well as with increasing chamber volume V . Figure 3 also illustrates the accuracy of the approximation by the very close agreement with a full numerical solution (dashed line).

Our model points to the crucial role that exsolved volatiles in the magma chamber play in controlling eruption volume and duration during effusive eruptions in which the eruption rate is controlled by the overpressure. As the effective compressibility of the magma increases, a given decrease in pressure leads to a greater expansion of the magma and therefore, for a given chamber size, a greater mass of magma is erupted. In turn, the density of the remaining gas–magma mixture is smaller, which leads to a smaller residual mass in the chamber. In addition, during such eruptions magma heating or cooling may also occur^{9,19,20}, especially after input of hot basaltic magma at the base of the chamber¹⁸. This brings in the last term on the right-hand side of equation (4). Heating and cooling lead to changes in magma crystallinity and in turn this can change the volatile saturation in the chamber (for example, $A \rightarrow B$, $C \rightarrow D$ in

Fig. 2c). Such changes in volatile saturation may greatly change the eruption rate. Figure 4 illustrates the increase in eruption rate that may occur as the magma is cooled against the country rock¹⁰ so that it eventually becomes saturated in volatiles owing to the additional crystallization. At this stage the compressibility increases by an order of magnitude (Fig. 2), the chamber pressure also increases owing to the exsolution and the timescale of the continuing eruption increases by a factor of ten.

Although our model is idealized, transitions in volatile saturation within a magma chamber may help to provide new explanations for the abrupt declines in eruption regimes, such as observed during dome eruptions at Mt Redoubt, Alaska²¹, in 1992, Mt Unzen, Japan⁵, in 1995 and at Soufrière Hills, Montserrat⁷, in 1998. In reality, flows in conduits are more complex than modelled here and may have multiple flow states^{16,17,22,23}. Our simple linear relationship (7) captures the behaviour on one solution branch and points to the dominant control of volatiles in the chamber on eruption longevity. Transitions from one steady state to a different solution branch can lead to more complex eruption histories and this needs to be considered alongside our analysis of phenomena that occur only in the magma chamber. The challenge now is to collect and interpret field data with the appropriate theoretical models in mind. □

Received 13 August; accepted 14 October 2002; doi:10.1038/nature01211.

1. Sigurdsson, H. (ed.) *Encyclopedia of Volcanoes* (Academic, San Diego, 2000).
2. Rose, W. I. Pattern and mechanism of volcanic activity at the Saniaguito volcanic dome, Guatemala. *Bull. Volcanol.* **36**, 73–94 (1972).
3. Rose, W. I. Volcanic activity at the Santiaguito volcano, 1976–1984. *Geol. Soc. Am.* **212**, 17–27 (1987).
4. Swanson, D. A. & Holcomb, R. T. *Lava Flows and Domes; Emplacement and Hazard Implications* (ed. Fink, J. H.) 3–24 (Springer, Berlin, 1990).
5. Nakada, S., Shimizu, H. & Ohta, K. Overview of the 1990–1995 eruption at Unzen Volcano. *J. Volcanol. Geotherm. Res.* **89**, 1–22 (1999).
6. Belousov, A., Belusova, B. & Voight, B. Multiple edifice failures, debris avalanches and associated eruptions in the Holocene history of Shiveluch volcano, Kamchatka, Russia. *Bull. Volcanol.* **61**, 324–342 (1999).
7. Sparks, R. S. J. & Young, S. R. *The Eruption of Soufrière Hills Volcano, Montserrat, from 1995 to 1999* (eds Druitt, T. H. & Kokelaar, B. P.) 45–69 (Memoir, Geological Society, London, 2002).
8. Blake, S. Volcanism and the dynamics of open magma chambers. *Nature* **289**, 783–785 (1981).
9. Blake, S. Volatile oversaturation during the evolution of silicic magma chambers as an eruption trigger. *J. Geophys. Res.* **89**, 8237–8244 (1984).
10. Tait, S., Jaupart, C. & Vergnolle, S. Pressure, gas content and eruption periodicity of a shallow, crystallising magma chamber. *Earth Planet. Sci. Lett.* **92**, 107–123 (1989).
11. Touloukian, Y. S., Judd, W. R. & Roy, R. F. *Physical Properties of Rocks and Minerals* Vol. 1 (McGraw Hill, New York, 1981).
12. Huppert, H. E., Turner, J. S. & Sparks, R. S. J. The effects of volatiles on mixing in calcalkaline magma systems. *Nature* **297**, 554–557 (1982).
13. Sparks, R. S. J. The dynamics of bubble formation and growth in magmas: A review and analysis. *J. Volcanol. Geotherm. Res.* **3**, 1–37 (1978).
14. Hurwitz, S. & Navon, O. Bubble nucleation in rhyolitic melts: Experiments at high pressure, temperature and water content. *Earth Planet. Sci. Lett.* **122**, 267–280 (1994).
15. Burnham, C. W. & Jahns, R. H. A method for determining the solubility of water in silicate melts. *Am. J. Sci.* **260**, 721–745 (1962).
16. Melnik, O. E. & Sparks, R. S. J. Non-linear dynamics of lava dome extrusion. *Nature* **402**, 37–41 (1999).
17. Barmin, A., Melnik, O. & Sparks, R. S. J. Periodic behaviour in lava dome eruptions. *Earth Planet. Sci. Lett.* **199**, 173–184 (2002).
18. Couch, S., Sparks, R. S. J. & Carroll, M. R. Mineral disequilibrium in lavas explained by convective self-mixing in open magma chambers. *Nature* **411**, 1037–1039 (2001).
19. Stasiuk, M., Jaupart, C. & Sparks, R. S. J. On the variations of flow rate in non-explosive lava eruptions. *Earth Planet. Sci. Lett.* **114**, 505–516 (1993).
20. Floch, A. & Marti, J. The generation of overpressure in felsic magma chambers by replenishment. *Earth Planet. Sci. Lett.* **163**, 301–314 (1997).
21. Miller, T. P. & Chouet, B. A. The 1989–1990 eruptions of Redoubt volcano—an introduction. *J. Volcanol. Geotherm. Res.* **62**, 1–10 (1994).
22. Jaupart, C. Gas loss from magmas through conduit walls during eruption. *Geol. Soc.* **289**, 783–785 (1998).
23. Massol, H. & Jaupart, C. The generation of gas overpressure in volcanic eruptions. *Earth Planet. Sci. Lett.* **166**, 57–70 (1999).

Acknowledgements We thank S. Sparks for comments and suggestions, and S. Blake and C. Jaupart for critiques on a first draft of this paper.

Competing interests statement The authors declare that they have no competing financial interests.

Correspondence and requests for materials should be addressed to H.E.H. (e-mail: heh1@esc.cam.ac.uk).